1521-009X/41/5/1082–1093$25.00
Drug Metabolism and Disposition

http://dx.doi.org/10.1124/dmd.112.048801
Drug Metab Dispos 41:1082–1093, May 2013

Metabolism of Bis(4-fluorobenzyl)trisulfide and Its Formation of Hemoglobin Adduct in Rat Erythrocytes

Hao Pan, Liqiang Gu, Siyuan Sun, Zhongjian Chen, Hui Zhou, Su Zeng, and Huidi Jiang

Department of Pharmaceutical Analysis and Drug Metabolism, College of Pharmaceutical Sciences, Zhejiang University, Hangzhou, China

Received September 5, 2012; accepted February 25, 2013

ABSTRACT

Bis(4-fluorobenzyl)trisulfide (BFBTS) is a promising new antitumor agent under investigation. It was metabolized rapidly in vivo in rat, but the metabolic fate and primary site of metabolism have not been clarified. In this study, we investigated the role of blood in the metabolism of BFBTS and compared the BFBTS metabolic potencies in whole blood, plasma, and red blood cells (RBCs) in vitro. Three major metabolites of BFBTS [bis(4-fluorobenzyl) disulfide, *para*-fluorobenzyl-mercaptan, and *para*-fluorobenzoic acid] were detected in RBCs and whole blood. Significant metabolism of BFBTS was observed in RBCs that were identified as the primary site of BFBTS metabolism. Thiols, including endogenous thiols and hemoglobin, were proven to be the critical factor in BFBTS metabolism. S-Fluorobenzylmercaptocysteine Hb (hemoglobin) adducts were characterized in vitro at BFBTS concentration of 250 μM and higher, whereas such Hb adducts were not detected in RBCs from Sprague-Dawley rats receiving a single intravenous injection of BFBTS at a high dose of 50 mg/kg. Liquid chromatography-tandem mass spectrometry results revealed that adduction induced by BFBTS was prone to take place at Cys125 of globin β chains. Otherwise, glutathionylation of Hb was also observed that may be attributed to the oxidative effect of BFBTS. In summary, BFBTS was unstable when it met with thiols, and RBCs were the main site of BFBTS metabolism. Hb adducts induced by BFBTS could be detected in vitro at high concentration but not in vivo even at high dose.

Introduction

Various naturally occurring sulfides have been demonstrated to have a lot of pharmacological effects, such as antibacterial, anticoagulative (Makheja and Bailey, 1990), antitumor (Wargovich et al., 1988; Sumiyoshi and Wargovich, 1990; Xiao and Singh, 2006; Iciek et al., 2007; Kim et al., 2007; Seki et al., 2008), antiradiation, antioxidative (Zeng et al., 2008), lipid-lowering effects (Warshafsky et al., 1993; Yeh and Yeh, 1994; Zhou et al., 2005), and some other important biologic activities (Agarwal, 1996; Amagase et al., 2001; Amagase, 2006). *Allium* vegetables are typical collection of those sulfides, to which consistent attention has been paid for their potential cancer preventive effects. It is widely investigated and well documented that diallyl trisulfide, a kind of trisulfide, is the primary antitumor component from garlic (Fukao et al., 2004; Xiao and Singh, 2006; Wang et al., 2012). Dibenzyl trisulfide (DBTS) is another well-documented trisulfide from a subtropical shrub, *Petiveria alliacea*, with potent antitumor activity (Rosner et al., 2001; Williams et al., 2004).

Bis(4-fluorobenzyl)trisulfide (BFBTS; Fig. 1), a novel trisulfide, is a synthetic analog of the sulfur-containing compound DBTS generated after a systematic screening against a wide range of tumor cell lines (An et al., 2006). BFBTS exhibits a broad spectrum of antitumor activity against nine human tumor cell lines and is more potent than DBTS (An et al., 2006). A further in vitro study reveals that BFBTS shows an equal antitumor potency between tumor cell lines overexpressing multidrug-resistant transporter gene, MDR1/ABCB1 (MCF7/adr and KBv2 cell lines), and their parental cell lines. The antiproliferation activity of BFBTS is mainly based on its inhibition on microtubule polymerization dynamics (Xu et al., 2009), while a further investigation reveals that BFBTS is covalently bound to β-tubulin at a novel site residue Cys12, forming β-tubulin-SS-fluorobenzyl. BFBTS also exhibits potent antitumor activity in nude mice bearing A549 lung cancer, Bcap-37 breast cancer, SKOV3 ovarian cancer, or MCF-7/adr breast cancer xenografts. The promising antitumor effects of BFBTS intrigue more efforts on its application as an agent for anticancer therapeutics.

Our previous study revealed the pharmacokinetic profile of BFBTS in rats (Gu et al., 2008). Similarly to the most widely investigated trisulfides (Sun et al., 2006), the concentration of BFBTS decreased rapidly within 30 minutes after its exposure to the circulation system, resulting in a short half-life in rat blood. A major metabolite bis(4-fluorobenzyl)disulfide (BFBDS) was detected in blood, having an equivalent exposure to the circulation system compared with its parent compound BFBTS. The final metabolites in rats were found to be *para*-fluorohippuric acid (*p*-FHA) and *para*-fluorobenzoic acid

The research was supported by National Major Special Project for Science and Technology Development of Ministry of Science and Technology of China [2011ZX11102].
dx.doi.org/10.1124/dmd.112.048801.

ABBREVIATIONS: BFBDS, bis(4-fluorobenzyl)disulfide; BFBTS, bis(4-fluorobenzyl)trisulfide; ESI, electrospray ionization; GC-MS, gas chromatography-mass spectrometry; GSH, reduced glutathione; Hb, hemoglobin; HPLC, high-performance liquid chromatography; IAI, iodoacetamide; LC-MS, liquid chromatography-mass spectrometry; LC-MS/MS, liquid chromatography-tandem mass spectrometry; *m/z*, mass-to-charge ratio; PBS, phosphate-buffered saline; *p*-FBA, *para*-fluorobenzoic acid; *p*-FBM, *para*-fluorobenzyl-mercaptan; *p*-FHA, *para*-fluorohippuric acid; RBCs, red blood cells; TOF, time of flight.

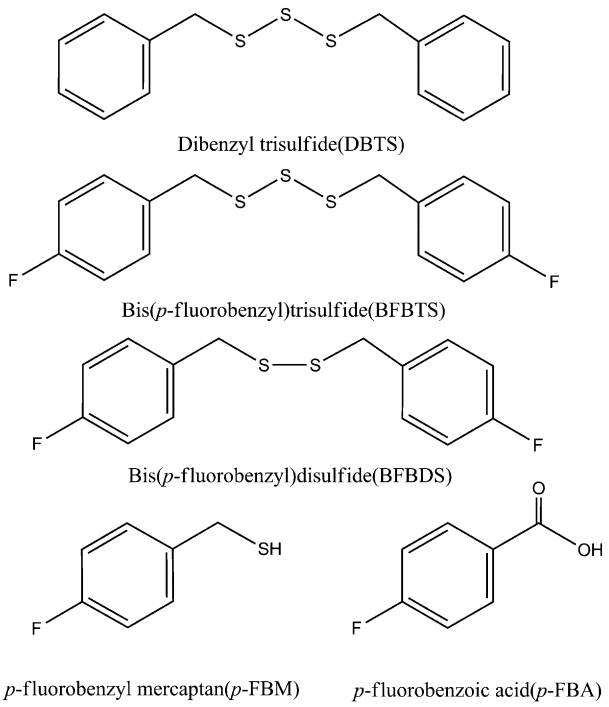

Fig. 1. Structures of BFBTS and its metabolites found in rat blood.

(*p*-FBA) (Pan et al., 2009). Although our previous studies suggested a possible complicated metabolism of BFBTS (Gu et al., 2008; Pan et al., 2009), the metabolic pathway and mechanism of BFBTS metabolism have not yet been clearly clarified.

On the basis of our preliminary study, BFBTS was shown to be much more unstable in blood than in liver microsomes, with an extremely short half-life in rat blood. Since the main route of BFBTS administration is the intravenous route, blood is probably critical in the disposition of BFBTS. In the current study, we investigated the factors involved in the significant metabolism of BFBTS in rat blood and identified the metabolites of BFBTS. As indicated in the literature (Hosono et al., 2005; Xu et al., 2009), the trisulfide might interact with the cysteine residues in biologic macromolecules, thus we confirmed the interactions between BFBTS and hemoglobin, the major protein in red blood cells. The results will contribute to a better understanding of the metabolic mechanism of BFBTS and other trisulfides in blood.

Materials and Methods

Materials

BFBTS, BFBDS, and *p*-fluorobenzyl-mercaptan (*p*-FBM) were provided by ACEA Bio Co., Ltd. (Hangzhou, China). *p*-FBA (purity 98.0%) was purchased from Sigma-Aldrich (Steinheim, Germany). Reduced glutathione and L-cysteine (purity >98.0%) were purchased from Sangon Biotech Co., Ltd. (Shanghai, China). *N*-acetyl-L-cysteine (purity >98%) was purchased from Sinopharm Chemical Reagent Co., Ltd (Shanghai, China). Trifluoroacetic acid (purity >99.5%) was purchased from Aladdin Industrial Inc. (Shanghai, China). Acetonitrile was of high-performance liquid chromatography (HPLC) grade from Tedia Co., Inc (Fairfield, OH). All other reagents were of analytical grade. The deionized water was purified by the Milli-Q Gradient A10 water system from EMD Millipore Corporation (Billerica, MA).

Animals

Male Sprague-Dawley rats (200–220 g) were obtained from Zhejiang Experimental Animal Center, Zhejiang Academy of Medical Science, Zhejiang, China. The certification number of the rats was SCXK (Zhe) 2003-0001. The rats were maintained on a 12-hour light/dark cycle and given water and fed ad libitum. All the procedures used in this study were approved by the Zhejiang University ethics committee.

In Vitro Metabolism of BFBTS in Blood

Preparation of Different Fractions of Rat Blood. Whole blood was collected from the orbital sinus of rats, the plasma was harvested after a centrifugation at 3,000 *g* for 10 minutes, and the red blood cells were washed with three volumes of isocratic phosphate-buffered saline (PBS) (pH 7.4) for three times and then resuspended in appropriate volume of PBS. BFBTS was incubated with whole blood and the two different fractions of blood for 2 hours, after liquid-liquid extraction and HPLC analysis, and the recoveries were compared for stability investigation.

Identification of BFBTS Metabolites in Rat Blood. BFBTS was incubated with rat whole blood, plasma, and red blood cells (RBCs) at 37°C. For the identification of metabolites, the reaction was terminated by rapid addition of two volumes of acetonitrile to the incubation system. The mixture was vortexed for 1 minute followed by centrifugation at 13,000*g* for 10 minutes, and the resultant supernatant was subjected to liquid chromatography-mass spectrometry (LC-MS) and gas chromatography (GC)-MS analysis.

Kinetics of BFBTS Metabolism in Rat Blood. For the kinetic study, BFBTS (final concentration, 50 μM) was incubated with RBCs diluted with equal volume of PBS or whole blood for designated time (5, 10, 15, 30, 45, and 60 minutes), and the substrate and metabolites were determined by the following methods. For metabolite M2 and M3 assay, two volumes of acetonitrile were added to the incubation system, and the samples were prepared by the method previously described, followed by HPLC analysis, while for BFBTS and metabolite M1 analysis, the samples were treated by the method reported (Bao et al., 2008; Gu et al., 2008). Briefly, 3 ml of extraction solvent (*n*-hexane:isopropyl alcohol = 95:5, v/v) was added to the incubation system, followed by liquid-liquid extraction for 5 minutes; the dried organic layer was reconstituted in mobile phase and subjected to HPLC analysis.

Profile of BFBTS Metabolism in Rat RBCs. The relation among the metabolites is critical for a better understanding of the BFBTS metabolism, especially the sequential metabolism; therefore, rat RBCs were incubated with all the different metabolites, respectively. After sample preparation by the method described in *Identification of BFBTS Metabolites in Rat Blood*, the supernatant was analyzed using HPLC. The metabolites were confirmed using the authentic standards.

Investigation of the Mechanism of BFBTS Metabolism

The Impact of Sulfhydryl Groups on the Metabolism of BFBTS. Reduced glutathione (GSH), cysteine, *N*-acetyl cysteine, and coenzyme A are the common endogenous thiols in biologic systems. BFBTS (final concentration, 5 μM) was incubated with 0.5 mM GSH, cysteine, *N*-acetyl cysteine, or coenzyme A, respectively, in PBS for 15, 30, and 60 minutes, followed by the liquid-liquid extraction and HPLC analysis as previously described.

To confirm the role of sulfhydryl groups in the metabolism of BFBTS, RBCs were preincubated with iodoacetamide (IAI; 5 mM), a classic thiol-residue blocking reagent, for 1 hour, after which BFBTS (final concentration, 5 μM) was added and incubated for another 1 hour. The mixture was treated as previously described, and a time-concentration profile of BFBTS was depicted to evaluate the effect of thiol group in the degradation of BFBTS.

Mechanism of Interaction between GSH and BFBTS. BFBTS (5 μM) was incubated with GSH (0.5 mM) in PBS (pH 7.4) for 30 minutes and two volumes of acetonitrile were added to the incubation system followed by HPLC and LC-MS analysis.

Chromatographic Conditions

HPLC-Ultraviolet Analysis of BFBTS and Its Metabolites. The HPLC analysis was performed using a Diamonsil C_{18} column (250 mm × 4.6 mm, 5 μm) with a C_{18} guard column (15 mm × 4.6 mm, 5 μm) at 30 ± 1°C. The analysis was carried out by a gradient mobile phase consisted of acetonitrile (A) and 0.1% phosphoric acid solution (B) at a flow rate of 1.0 ml•min^{-1} (0–7 minutes 25% A and 75% B, 13–25 minutes 85% A and 15% B). The diode

array detector was set at a wavelength of 220 nm for determination of BFBTS, BFBDS, and *p*-FBM and 230 nm for *p*-FBA.

GC-MS Analysis of *p*-FBM. Capillary GC-MS analysis was carried out on a 6890N/5975 Inert GC-MS instrument (Agilent Technologies, Santa Clara, CA) equipped with a data processing system (Agilent ChemStation system). Gas chromatography was performed on an HP-5MS capillary column (30 m × 0.25 mm i.d.) with the stationary (bonded 5% phenyl and 95% dimethylpolysiloxane) coated at a 0.25 μm film thickness. High purity helium (99.99%) was used as the carrier gas at a constant flow rate of 1 ml•min^{-1} maintained by an electronic pressure controller. A split/splitless injection system operated in the split mode was used, and the split ratio was set at 10:1. The injector and interface temperatures were set at 250 and 280°C, respectively. The oven temperature was programmed from 80 to 180°C at the rate of 6°C•min^{-1} and then held for 10 minutes, increased to 250°C at 10°C•min^{-1} and held at 280°C for 5 minutes. The mass spectrometer was operated in the electron impact mode at the energy of 70 eV, and the ion source temperature was set at 200°C. The mass spectra were recorded in full scan mode to collect the total ion current within the *m/z* (mass-to-charge ratio) range from 50 to 500.

UPLC-MS Analysis of *p*-FBA. The UPLC-MS analysis was performed on a ultra-performance liquid chromatography ACQUITY instrument (Waters, Milford, MA) equipped with a triple quadrupole detector. LC-MS analysis was performed on an ACQUITY ultra-performance liquid chromatography BEH C_{18} column (2.1 × 100 mm × 0.17 μm) under negative ion mode. The flow rate of mobile phase was 0.2 ml•min^{-1} and the gradient elution programmed from 75% A (0.1% formic acid)/25% B (acetonitrile): at 0–1 minute to 25% A/75% B at 11–13 minutes. The column temperature was controlled at 25°C during the analysis. Capillary voltage: 3.30 kV, cone voltage: 31 V, source temperature: 150°C, desolvation temperature: 350°C were set for MS analysis.

Investigation of BFBTS-Induced Hemoglobin Adducts

In Vitro Incubations of BFBTS with RBCs. The collected RBCs were resuspended in nine volumes of PBS (pH 7.4) before incubation with BFBTS (5 μM and 200 μM, final concentrations) in a metabolic shaking bath for 0.5 hour at 37°C and the globins were isolated using acidified acetone after incubation as the method described previously (Moll et al., 2000). Briefly, 6 volumes of cold acidified acetone (1% HCl) were added to the incubation system to precipitate the globins. The sample was centrifuged at 3,000 *g* for 10 minutes, and then the pellets were washed with cold acidified acetone, cold acetone, and cold diethyl ether, successively. The globins were dried under vacuum and kept at −20°C.

In Vivo Study of BFBTS-Derived Hemoglobin Adducts. For in vivo study of hemoglobin adducts, three male rats were administered a single injection intravenously a dose of BFBTS (50 mg/kg, 8-folds of the effective dose), and the heparinized whole blood was collected at 30 minutes postdose because the rapid elimination phase of BFBTS in vivo was estimated to be 30 minutes (Gu et al., 2008). The heparinized whole blood was processed immediately to obtain globins as previously described. The control globins were also obtained from the blood harvested pre-dose.

Electrospray Ionization/Mass Spectrometry Analysis of Intact Globin Chains. Acetone precipitated globins were dissolved in acetonitrile: H_2O (50:50) before analysis on liquid chromatography-hybrid quadrupole time-of-flight mass spectrometry (TOF)-LC (ABSciex; API QSTAR). The spectra were scanned with a mass range 200–1500 *m/z*, and series of multiply charged ions were deconvoluted using Analyst software (Applied Biosystems, Foster City, CA).

Trypsinization of Hemoglobin. Hemoglobin (Hb) from RBCs incubated with 50 or 500 μM BFBTS along with their respective controls were trypsinized for modified peptide analysis. Proteolytic digestion of precipitated Hb samples was carried out in 100 mM ammonium bicarbonate (pH 8.4) at 37°C for 20 hours. The reaction was stopped by adding trifluoroacetic acid to bring the solution to pH < 3 prior to analysis by LC/electrospray ionization (ESI)/MS.

Mass Spectrometry. Tyripsinized samples of globins from control RBCs and RBCs exposed to BFBTS were loaded onto a Zorbax 300-SB C_{18} trap column for online desalting and sample cleanup, followed by separation on RP-C_{18} column (0.150 mm × 15 mm, 300 Å; Column Technology Inc., Fremont, CA) and analyzed using linear trap quadrupole Velos Dual-Pressure Ion Trap Mass spectrometer (Thermo Fisher Scientific Inc., Rockville, MD). The LC method was as follows: mobile phase A was 0.1% formic acid in H_2O and mobile phase B was 0.1% formic acid in 84% acetonitrile. Peptides were eluted with a linear gradient of mobile phase. The mobile phase B was increased from 4 to 50% during 0 to 50 minutes and then increased to 100% over 4 minutes and held for another 6 minutes. As peptide was eluted and injected into the LC/ESI source, 20 MS/MS spectra were collected after every MS scan. Customized database was created after import of the Sprague-Dawley rat Hb amino sequence (α1, β1, β2, β3, β4) (Ferranti et al., 1993). Raw MS/MS data were used to search for a rat Hb peptides modifications in a customized amino acid sequence using Bioworks and SEQUEST program (Thermo Fisher Scientific Inc.).

Results

Identification of BFBTS Metabolites in Rat Blood after In Vitro Incubation

As BFBTS was found to be extremely unstable in rat blood, we identified the metabolites to clarify the metabolic fate of BFBTS. BFBTS (50 μM) was incubated with rat blood for 15 minutes followed by HPLC analysis to identify metabolites. BFBTS and three metabolites were detected, which were well separated in the liquid chromatography (Fig. 2.).

By GC/MS analysis, we found M1 and M2 shared the same spectra with the authentic standards of BFBDS and *p*-FBM, respectively (Fig. 3). In the MS analysis of M1, the [M] ion of 282 represented BFBDS, while fragmental ion *m/z* 109 and 83 represented the [*para*-fluorobenzyl] and [FC_5H_4], respectively. While in the MS analysis of M2, the [M] ion of 141.8 represented *p*-FBM, and fragmental ion *m/z* 95 and 83 represented the [M-CH_2SH] and [M-C_2H_2SH], respectively.

After UPLC-MS/MS analysis, identical spectra of M3 and *p*-FBA were observed (Fig. 3). In the MS spectrum, the parent ion of M3 was 139, which represented the [M-H]$^-$, meanwhile, the characteristic structure of BFBTS-derived metabolite was the *p*-fluorobenzen ring, which was represented by ion *m/z* 95.

M1 was finally confirmed to be BFBDS after comparing the retention time of metabolite with the corresponding authentic standard, and it was also the major metabolite identified in our previous pharmacokinetic study of BFBTS (Gu et al., 2008). The retention times of M2 and M3 were also identical with the authentic standards of *p*-FBM and *p*-FBA, respectively.

On the basis of the above results, we identified the M1, M2, and M3 as BFBDS, *p*-FBM, and *p*-FBA, respectively.

The Identification of Major Metabolic Site and Mechanism of the BFBTS Metabolism

The Kinetic Profile of BFBTS Metabolism in Rat Whole Blood and RBCS. For the identification of the main metabolic site, the stabilities of BFBTS in different fraction of rat blood were compared. The recovery of BFBTS (64 μM) in rat whole blood and plasma after incubation for 2 hours was 2.54 and 12.98%, respectively, whereas no BFBTS was retained in RBCs. The kinetic study was conducted based on the time-concentration profile of BFBTS metabolism in rat RBCs, and the time-concentration profile of BFBTS metabolites was also depicted (Fig. 4). A rapid elimination of BFBTS coupled with a rapid formation of M2 (*p*-FBM) was observed. The formation of M3 (*p*-FBA) was relatively slow and steady in comparison with M2. The characteristics of metabolites formation were consistent in RBCs and whole blood, which strongly indicated that RBCs play a more important role in the elimination of BFBTS. Appropriately diluted RBCs (10 e^8/ml) were used to estimate the metabolism of BFBTS. The estimated half-life of BFBTS in RBCs was less than 0.5 minute by nonlinear-regression method using GraphPad Prism 5.0 (GraphPad Software, La Jolla, CA).

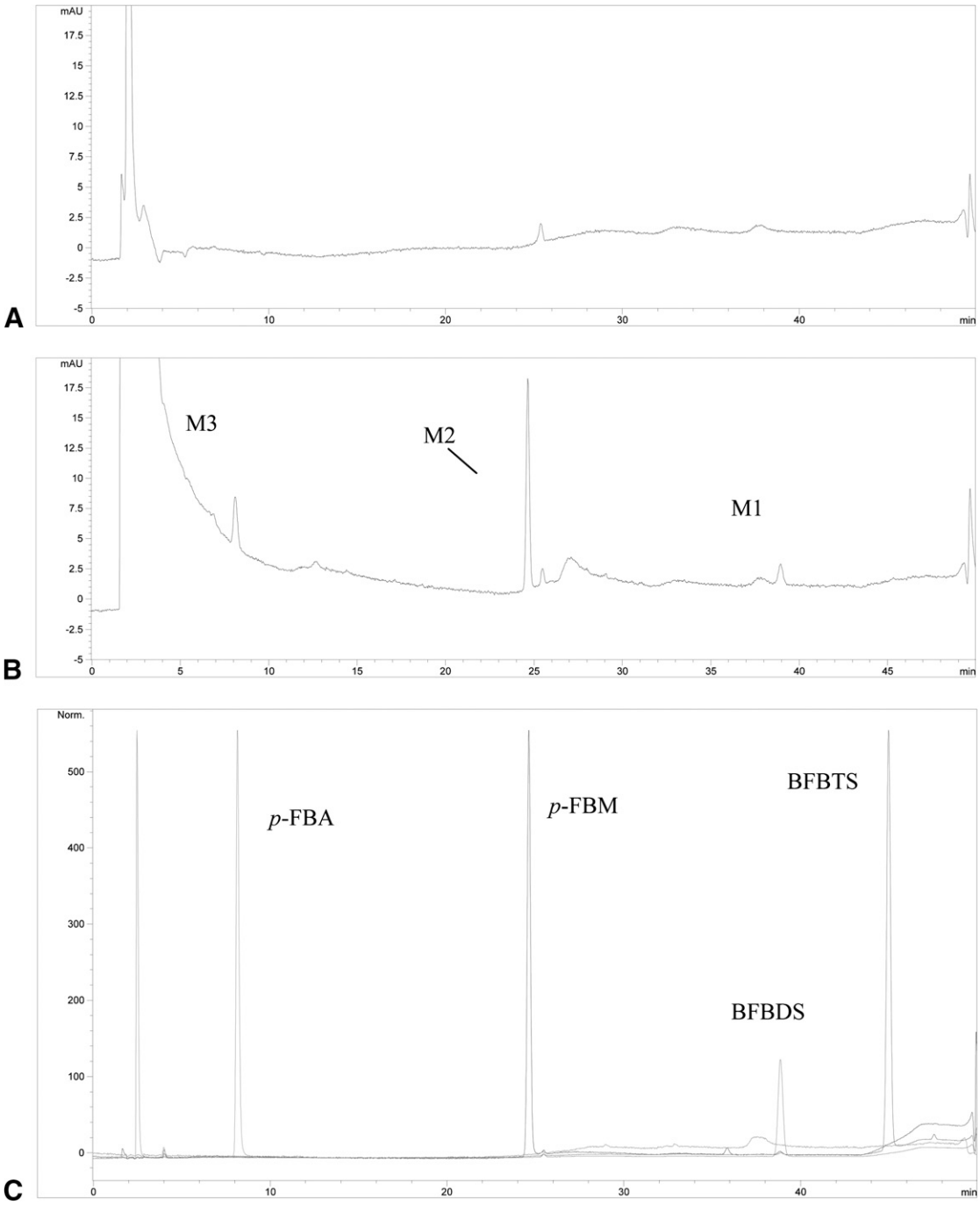

Fig. 2. Representative HPLC chromatograms. (A) Blank blood sample; (B) Samples at 15 minutes after incubation of BFBTS (50 μM) with the whole blood from rats. Three metabolites were detected after comparing the retention time with authentic standards of *p*-FBA, *p*-FBM, and BFBDS (C) [(1) *p*-FBA, retention time: 8.15 minutes; (2) *p*-FBM, retention time: 24.66 minutes; (3) BFBDS, retention time: 38.89 minutes].

Involvement of the Thiol Group in BFBTS Metabolism. It was known that thiol-exchange reactions may occur between thiols and disulfide bond. Thus, a series of endogenous thiols were investigated and compared with determine the main metabolic contribution in blood. BFBDS and *p*-FBM were detected after incubation of BFBTS with GSH, Cys, *N*-acetyl cysteine, and coenzyme A, and the time profile of BFBTS metabolism was shown in Fig. 5. BFBTS was unstable when it was exposed to all the small molecules containing sulfhydryl group. After 30-minute incubation, BFBTS was almost undetectable. In RBCs, the endogenous thiols were reported to be abundant (~2 mM) (Di Simplicio et al., 1998), which may contribute to the metabolism of BFBTS. Notably, such fast elimination of BFBTS in RBCs was almost completely inhibited when RBCs was preincubated with IAI, which reacted with thiol and significantly blocked most of the exposed thiol residues (Fig. 5). The above results strongly indicated a significant involvement of thiols in BFBTS metabolism in RBCs.

Minor potential GSH-*p*-FBM conjugate can be detected after 30-minute incubation of BFBTS in GSH system using LC-MS. Briefly, the precursor ions of the conjugate were 448 and 470, which were

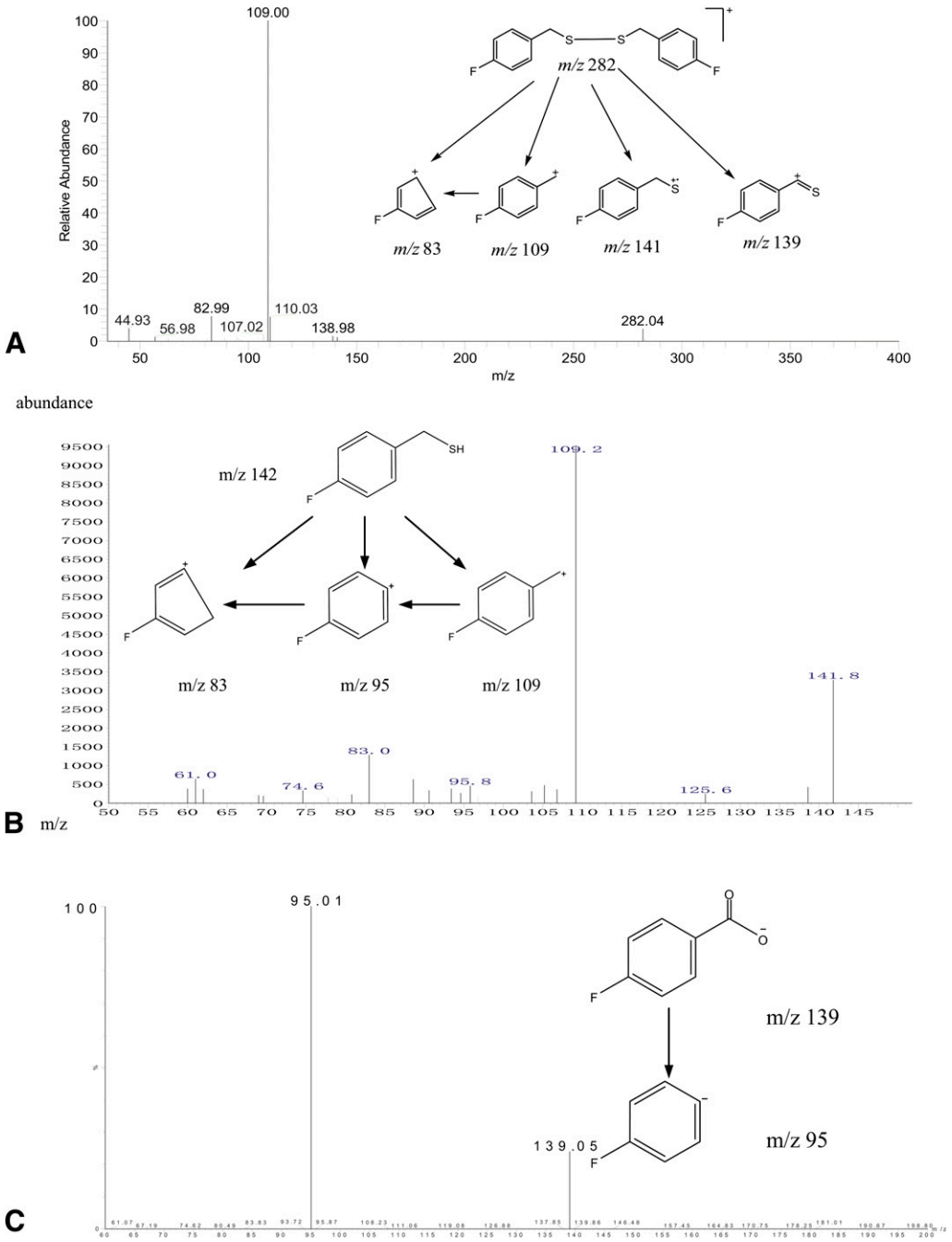

Fig. 3. MS spectra of metabolites M2 and M3 found in rat blood after in vitro incubation with BFBTS. The pattern of fragmentation was illustrated: BFBDS (A), *p*-FBM (B), and *p*-FBA (C).

identified to be the $[M+H]^+$ and $[M+Na]^+$ ion of GSH-*p*-FBM, and their corresponding product ions were 306 and 328, which can be the fragment generated by losing *p*-FBM. This observation indicated a direct thiol exchange reaction between BFBTS and GSH, which generated an unstable intermediate, GSH-*p*-FBM. The reaction mechanism was proposed in Fig. 6, the generation of H_2S was confirmed using Lead(II) acetate paper test.

Sequential Metabolism of BFBTS in Rat RBCs and Metabolism of BFBTS in Different Fractions of Rat Blood. After comparing the metabolic profile of BFBTS, M1, M2, and M3 in rat RBCs, the observation was summarized in Table 1. The results indicated a complicated sequential metabolism. A reversible reaction existed between M1 and M2, and M3 was the terminal metabolite of BFBTS in rat RBCs.

The metabolism of BFBTS in different fractions of rat blood was also investigated. M1 and M2 were both detected from all the incubation systems, whereas M3 was only found in rat whole blood and rat RBCs. Collectively, M3 is the terminal product of BFBTS metabolism in rat blood, and rat RBCs are the only site where M3 is generated

In Vitro Study of BFBTS-Induced Modification of Rat Hemoglobin

ESI-TOF Analysis of Intact Globin. Another major part of endogenous thiols in RBCs are the macromolecules with cysteine (thiol) residues, among which hemoglobin is the most abundant.

Assessing hemoglobin adducts is also toxicologically important, as it can be used to indicate enzyme inhibition or the physiology of hemoglobin may be altered after modification (Eyer et al., 1983). ESI-TOF is a useful tool to investigate macromolecules based on its accurate mass. Thus, the interaction of BFBTS with hemoglobin was investigated using ESI-TOF. Fresh isolated rat RBCs were incubated with 1, 10, 50, 250, and 500 μM BFBTS, 250 μM BFBDS, and 500 μM *p*-FBM at pH 7.4, 37°C for 30 minutes. After globins were acetone precipitated and isolated, samples were subjected to ESI/MS for intact protein analysis. The presence of adducts was determined on the basis of a mass shift of the unmodified chain, because the sulfur-sulfur bond can be easily broken up and form new sulfur-sulfur bond with sulfhydryl groups. The theoretical adducted moiety was *p*-FBM, thus, the theoretical mass shift was +140 Da for mono-adduct of *p*-FBM moiety and +280 Da for bis-adduct. Our analysis of all incubation revealed the presence of mono-adduct on both α1 and β2 chain of Hb when the concentration of BFBTS was above 250 μM, while a significant glutathionylation on β chain was also observed (Fig. 7). The Hb adducts were undetectable when BFBTS concentrations were lower than 250 μM, which was due to the elimination mediated by small thiols. However, no Hb adducts were detected when RBCs were incubated with BFBDS or *p*-FBM at high concentration.

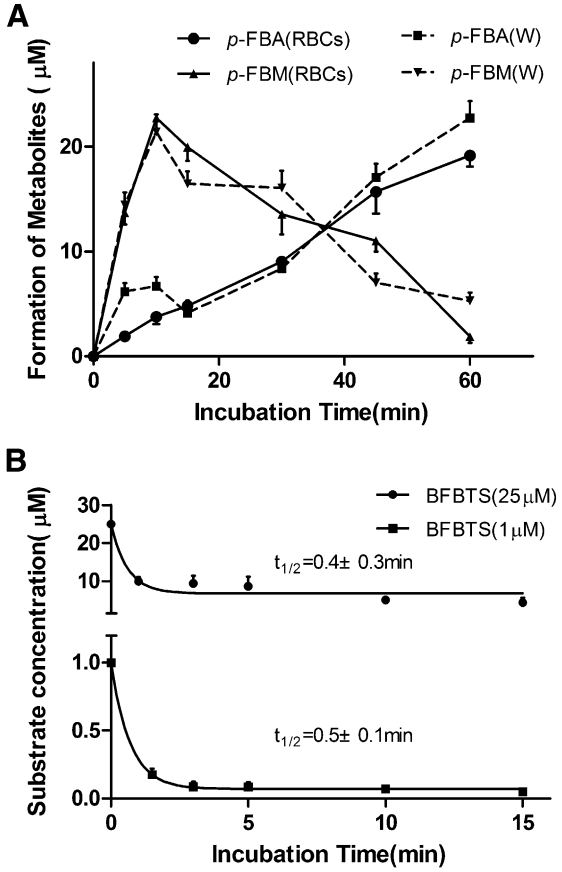

Fig. 4. The concentration-time profiles of BFBTS and its metabolites in RBCs. (A) BFBTS (50 μM) was incubated with RBCs and whole blood for 5, 10, 15, 30, 45, 60 minutes. After termination by adding two volumes of acetonitrile, the formation of BFBTS metabolites (M2, *p*-FBM; M3, *p*-FBA) were analyzed by HPLC. (B) BFBTS was incubated with diluted RBCs ($10e^8$/ml) for short time (1.5, 3, 5, 10, 15 minutes). After extraction, BFBTS was analyzed by HPLC, and the time-concentration profile of BFBTS metabolism in RBCs is depicted. The half-life of BFBTS was calculated by nonlinear regression using GraphPad 5.0 (data points represent the means; n = 3; and standard deviation was applied).

Liquid Chromatography-Tandem Mass Spectrometry (LC-MS/MS) Analysis of Peptide Digestion. On the basis of the published reports (Hosono et al., 2005) and our results, cysteine residues were expected to be the modified sites. It was known that there are three cysteine residues on the α chain (Cys13, Cys104 and Cys111) and two on the β chain (Cys93 and Cys125) in Hb, so we carried out LC-MS/MS analysis of Hb peptides to determine the major modification site. Briefly, the globin samples from vehicle control and 250 and 500 μM BFBTS-treated rat RBCs were trypsinized and subjected to LC-MS/MS analysis using linear trap quadrupole Velos Dual-Pressure Ion Trap Mass spectrometer.

The globins from 250 μM BFBTS-treated RBCs revealed three BFBTS-modified peptides (Table 1). Cys104/Cys111-containing peptide (α1 93–126) and Cys125-containing peptides (β2/β3 105–132) were both identified as BFBTS adducts. The MS/MS fragmentation patterns of Cys104-containing peptides and Cys125-containing peptides were consistent with the BFBTS adducts at the cysteine residue (Fig. 8). The spectrum of triple-charged precursor ion (m/z 1059.22) referring to the modified Cys125-containing peptide displayed five b ions and ten y ions. The fragmentation between Thr123 and Pro124 gave rise to a single-charged y9 ion (1103.48) and a double-charged b19 ion (1139.98), while the high intensity of double-charged y21 ion (1218.33) along with the presence of corresponding double-charged b7 ion (371.30) were due to the fragmentation between Val111 and Ile112. All the above results suggested the presence of BFBTS on the cysteine-containing fragment of these peptides.

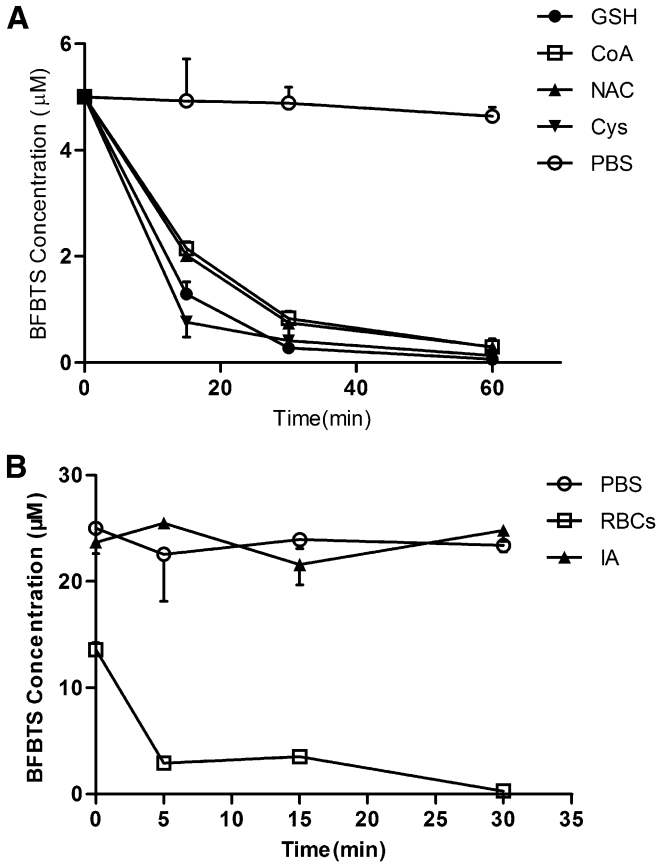

Fig. 5. Involvement of thiols in BFBTS elimination in RBCs. The concentration-time profile of BFBTS (5 μM) elimination by thiols (A) and the inhibition of BFBTS (25 μM) elimination in RBCs after preincubation with IAI (5 mM). (B) Stability of BFBTS in PBS was taken as control (data points represent the means; n = 3; and standard deviation was applied). CoA, coenzyme A; NAC, *N*-acetyl-cysteine.

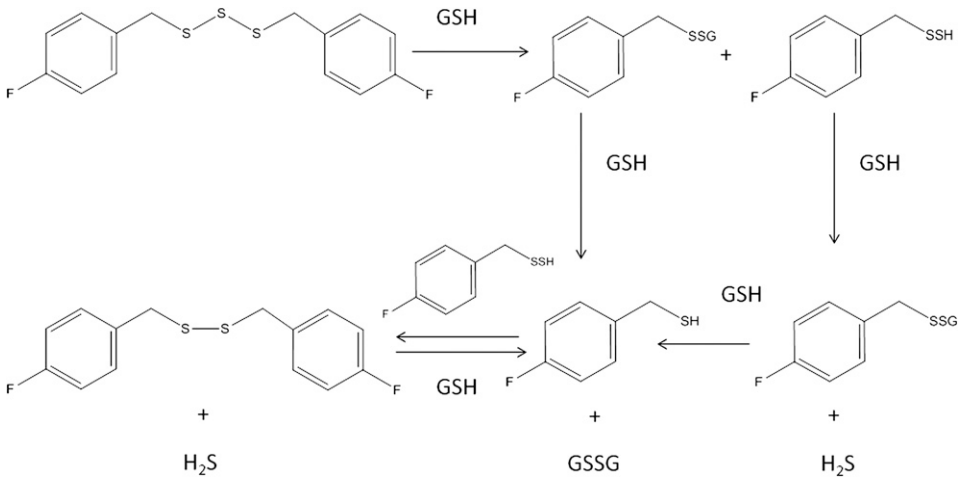

Fig. 6. Proposed mechanism of BFBDS and *p*-FBM formation.

The globins isolated from RBCs treated with 500 μM BFBTS revealed a more wide modification on cysteine-containing peptides, and eight BFBTS-modified peptides were detected (Table 2) including Cys104/Cys111-containing peptide (α1 100–127), Cys93-containing peptide (β1/β2/β3/β4 83–95, 83–104), and Cys125-containing peptide (β1 121–132, β2/β3 121–132, β2/β3 105–132, 121–146). The Cys125-containing peptides 121–132 on the β1 chain and 121–132, 105–132, and 121–146 on the β2/β3 chain were detected to be modified by BFBTS after confirming the MS/MS fragmentation pattern. The results also revealed the BFBTS adducts on the cysteine residues of Cys104/Cys111-containing peptide 100–127 from the α1 chain and Cys93-containing peptides 83–95 and 83–104 from β1/β2/β3/β4. The MS/MS data of trypsin digested globins from incubation system of BFBTS at 250 and 500 μM revealed the wide involvement of Cys125 from β1/β2/β3 chain and high reactivity toward BFBTS.

In Vivo Study of BFBTS Modification of Rat Hb. To test whether such BFBTS-derived Hb adducts were formed in vivo, globins were isolated from collected rat blood at 30 minutes after a single i.v. injection of BFBTS at a dose of 50 mg/kg. By ESI/MS analysis, no difference was observed between globin samples from rat blood of predose and postdose (Fig. 9), which meant no formation of Hb adducts in vivo even at such a high dose.

Discussion

In this study, we investigated the metabolic pathway and the metabolic profile of BFBTS. The results showed that BFBTS was significantly metabolized in rat blood, especially in the RBCs, and generated three metabolites that were identified as M1: bis(4-fluorobenzyl)disulfide, M2: *para*-fluorobenzyl-mercaptan, and M3: *para*-fluorobenzoic acid. Our further in vivo study also confirmed the formation of BFBDS, *p*-FBM, and *p*-FBA in rat blood after i.v. injection of BFBTS. It was the first time to elucidate the metabolic fate of such a trisulfide compound in a biologic system.

The metabolism of BFBTS was dramatically rapid, coupling with the formation of BFBDS, *p*-FBM, and *p*-FBA in rat blood especially in rat RBCs. The time-concentration profiles of *p*-FBM and *p*-FBA formation in rat whole blood and RBCs showed no significant difference, which indicated the critical role of RBCs in the metabolism BFBTS. Moreover, the metabolism of BFBTS was extremely rapid even in a diluted RBCs suspension, therefore, it could be deduced that the RBCs was the primary metabolic site of BFBTS metabolism.

Incubation of BFBTS, M1, and M2 all generated *p*-FBA in rat RBCs, thus it could be concluded that *p*-FBA was the terminal metabolite in rat blood while *p*-FBM and BFBDS were the major intermediate metabolites. Our previous excretion study revealed that *p*-FBA and *p*-FHA were the major metabolites detected in rat urine (Pan et al., 2009), and it was commonly known that hippuric acid was formed by the conjugation of benzoic acid with glycine in mitochondria (Simkin and White, 1957). Thus, the reason why *p*-FHA was not detected in the in vitro incubation system or in vivo is probably that RBCs have no mitochondria.

Plasma did not exhibit a comparable metabolic potency, and *p*-FBA was also not generated in plasma, thus RBCs were also confirmed as the primary site of BFBTS metabolism in the aspect of terminal metabolite formation.

GSH and cysteine are the major endogenous thiols that keep the intracellular redox potential (Schafer and Buettner, 2001; Giustarini et al., 2008; Kemp et al., 2008), while coenzyme A and *N*-acetyl cysteine are the two thiols in the biologic systems with low concentration. Our investigation on the metabolic mechanism of BFBTS showed that the endogenous thiols were potent to transfer BFBTS to BFBDS and *p*-FBM. Since the concentration of GSH was relatively high (~2 mM) in RBCs, it was probable that GSH dominated the metabolism of BFBTS in rat blood. On the other hand, the total inhibition of BFBTS elimination after preincubation of RBCs with IAI confirmed the critical role of thiols.

The metabolism of BFBTS was presumed to be based on the fast thiol/disulfide (SH/SS) exchange (Iversen et al., 2010) and the high reactivity of BFBTS toward thiols due to its specific structure. A minor GSH conjugate was observed when BFBTS was incubated with GSH, which partially confirmed the previous hypothesis. *p*-FBA was not found in those thiol incubation systems, thus the formation of *p*-FBA was related to other mechanisms that should be further investigated.

Most of the studies about polysulfide metabolism are focused on disulfide and the hepatic metabolism system (Teyssier et al., 1999;

TABLE 1

Investigation of sequential metabolism of BFBTS in rat RBCs

Metabolite	Substrate			
	BFBTS	BFBDS	*p*-FBM	*p*-FBA
BFBTS	/	—	—	—
BFBDS	+	/	+	—
p-FBM	+	+	/	—
p-FBA	+	+	+	/

—, Not detected; +, detected; /, in such case, the metabolite is used as substrate

Teyssier and Siess, 2000; Germain et al., 2003), which is probably not critical for the metabolism of trisulfide. Apart from the endogenous thiols, the concentration of protein-SH groups is even higher in RBCs (Di Simplicio et al., 1998), which indicates the possible formation of covalent protein adducts.

Hemoglobin constitutes more than 95% of the protein content in the RBCs and contains more than one reactive cysteine residue (Di Simplicio et al., 1998). Moreover, some cysteine residues in rat hemoglobin have been demonstrated to be more reactive than the metabolically important thiols, such as GSH (Rossi et al., 1998). Hemoglobin adducts are also used widely to indicate or account for the potential toxicity-like enzyme inhibition (Zimmerman et al., 2002). Thus it is necessary to investigate the interaction between BFBTS and hemoglobin by assessing the formation of hemoglobin adducts.

Our in vitro study showed that BFBTS-derived adducts only formed at high concentrations (250 and 500 μM). The finding of no Hb adducts induced by BFBDS or *p*-FBM indicated the formation of Hb

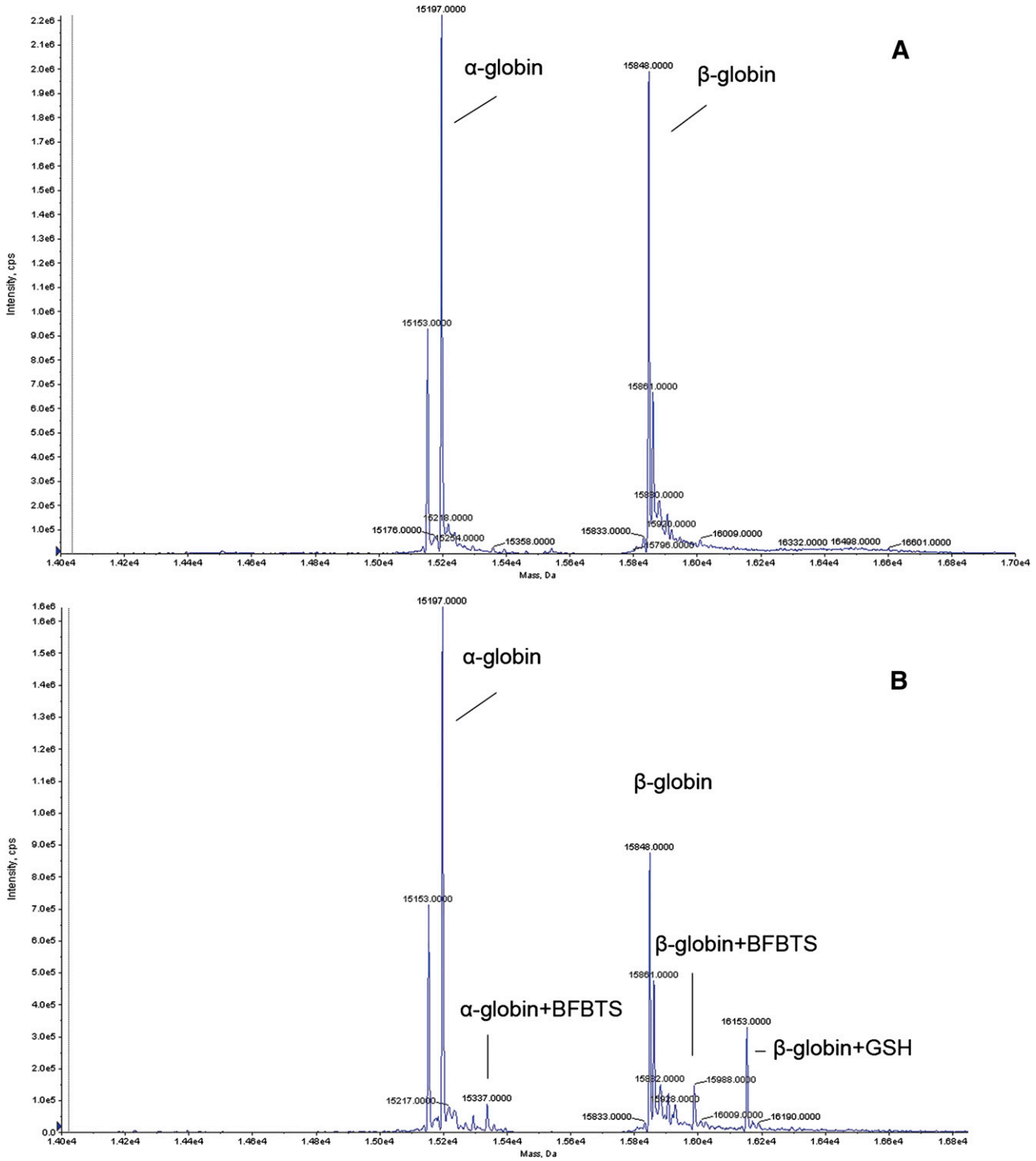

Fig. 7. ESI-Q-TOF analysis of intact globin. (A) Globins after incubation without BFBTS; (B) globins after in vitro incubation with BFBTS at 250 μM with three major Hb adduct formations detected.

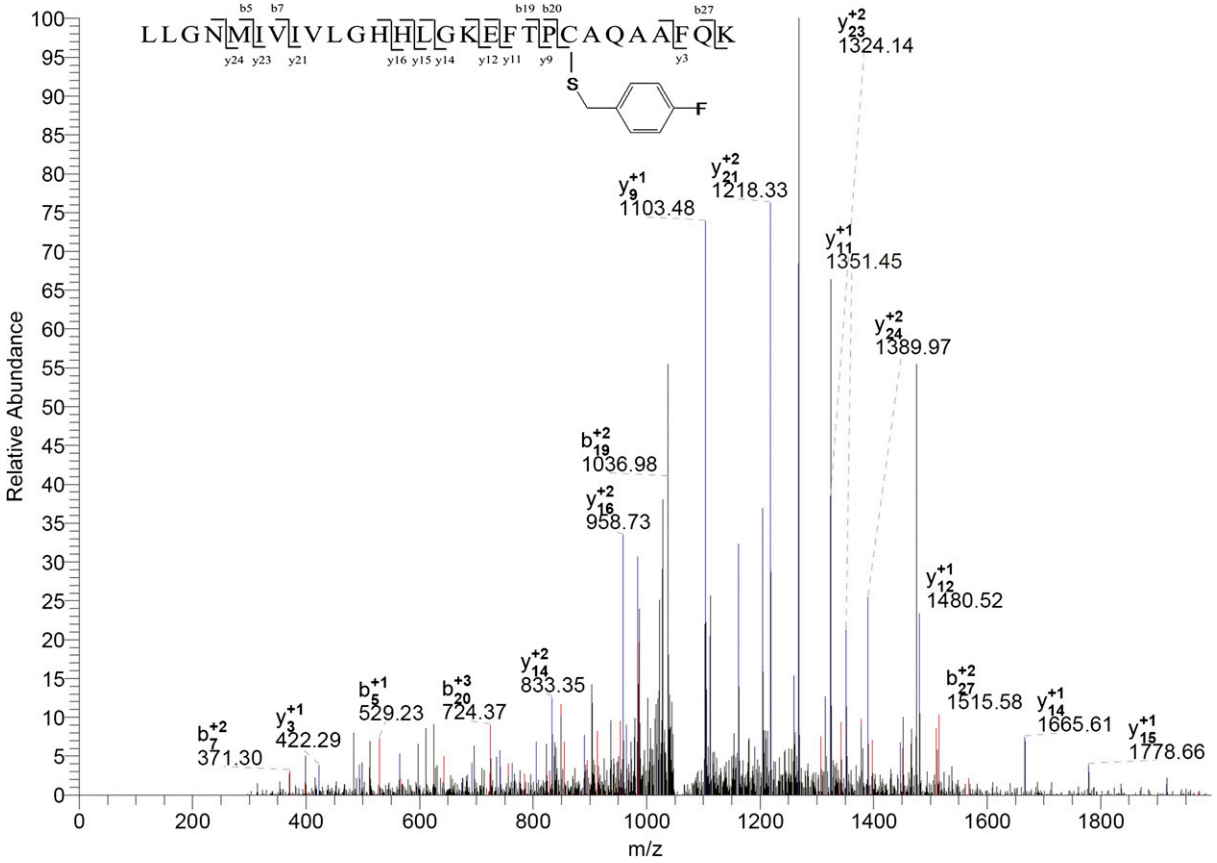

Fig. 8. LC-MS/MS of peptide β2/3 105-132 modified by BFBTS at Cys125.

adducts was based on thiol/disulfide exchange, and the structure of trisulfide meant higher reactivity toward thiols. The reason why BFBTS-derived adducts were not detected at low concentration was probably due to the great abundance of GSH in RBC (~2 mM) of rats (Guan et al., 2003). Our previous data revealed the rapid metabolism of BFBTS by GSH even at low concentration. Thus, the significant metabolism of BFBTS by GSH might have occurred before BFBTS getting access to Hb.

The detection of mono Hb adducts at high concentration (250 and 500 μM) by ESI-TOF was further supported by analysis of trypsin-digested globin, which revealed a modified Cys125-containing peptide on β1 chain at both concentrations of BFBTS (250 and 500 μM). And the modifications of Cys93 on β chain and Cys104/111 on α chain were detected at high concentration (500 μM).

BFBTS-derived mono-adducts at 4 out of 5 cysteine sites of the rat Hb were observed at high BFBTS concentration, whereas no multi-adducts were detected by ESI-TOF. This result may be ascribed to the low concentration of the potential multi-adducts and low sensitivity of ESI-TOF mainly caused by ion suppression when analyzing complex samples.

Cys125 is the obvious target because it is located externally at the α1/β1 interface of Hb (John, 1982). The exposure level of Cys125

TABLE 2

Peptides modified by the adducts of *p*-FBM moiety (+140.02 Da) after incubation of RBCs with BFBTS (250 and 500 μM)

Hb Chain	Peptide	Sequence	$Mass_{theo}$	$Mass_{obs}$	Modified Position
			Da	*Da*	
250 μM BFBTS					
α1	93-126	VDPVNFKFLSHCLLVTLACHHPGDFTPAMHASLD	4001.08	4001.00	104
α1	93-126	VDPVNFKFLSHCLLVTLACHHPGDFTPAMHASLD	4001.08	4000.96	111
β2/3	105-132	LLGNMIVIVLGHHLGKEFTPCAQAAFQK	3175.81	3175.66	125
500 μM BFBTS					
α1	100-127	FLSHCLLVTLACHHPGDFTPAM*HASLDK	3219.59	3219.02	104
α1	100-127	FLSHCLLVTLACHHPGDFTPAM*HASLDK	3219.59	3219.61	111
β1/2	83-95	GTFAHLSELHCDK	1598.64	1597.88	93
β1/2/3/4	83-104	GTFAHLSELHCDKLHVDPENFR	2706.86	2706.13	93
β1	121-132	EFSPCAQAAFQK	1467.51	1467.32	125
β2/β3	121-132	EFTPCAQAAFQK	1481.54	1480.76	125
β2/β3	105-132	EFTPCAQAAFQKVVAGVASALAHKYH	2886.16	2885.90	125
β2/β3	121-146	LLGNMIVIVLGHHLGKEFTPCAQAAFQK	3177.66	3177.49	125

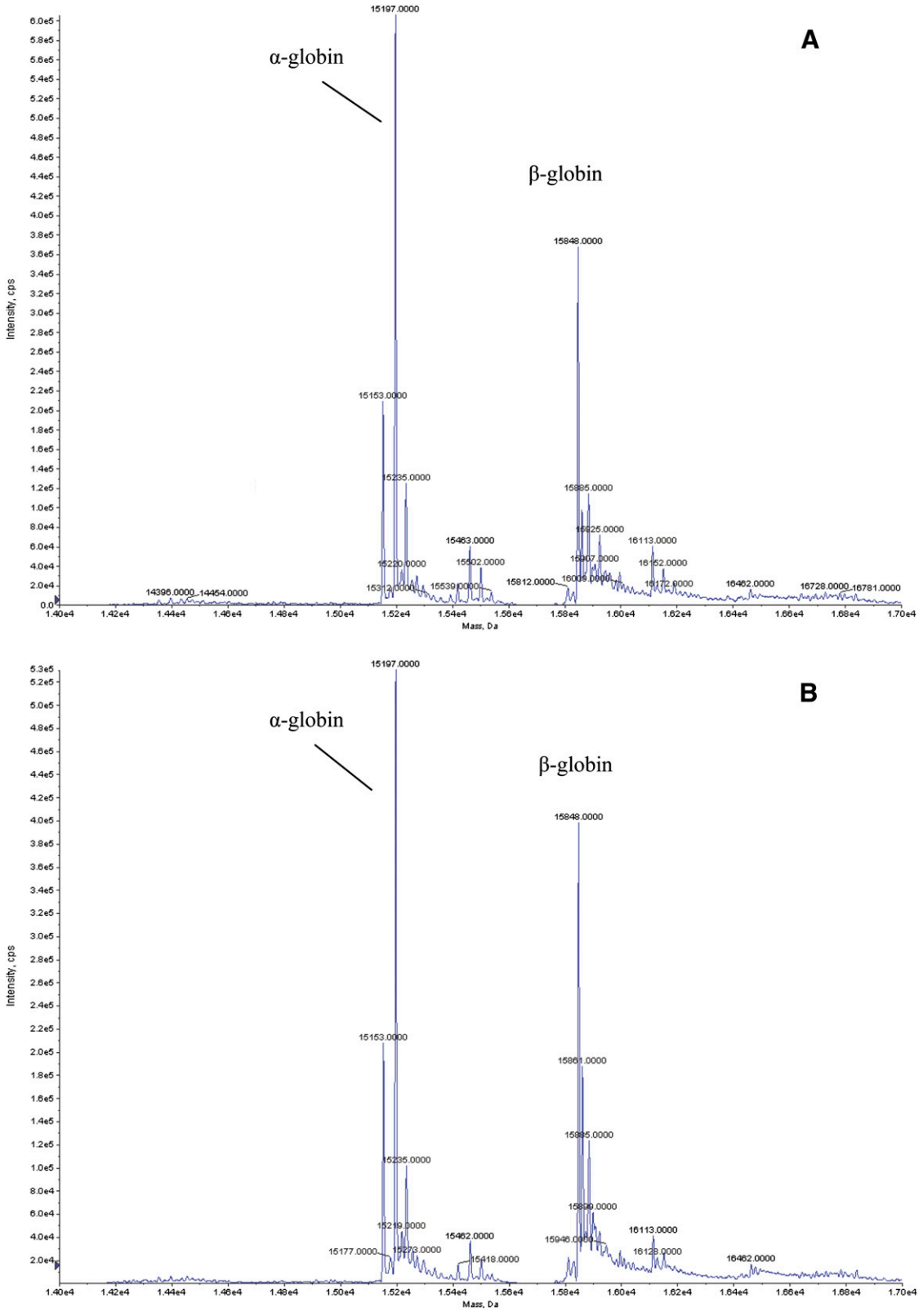

Fig. 9. ESI-Q-TOF analysis of intact globin. (A) Globin from Sprague-Dawley rat before administration; (B) Globin from Sprague-Dawley rat 30 minutes after administration (50 mg/kg).

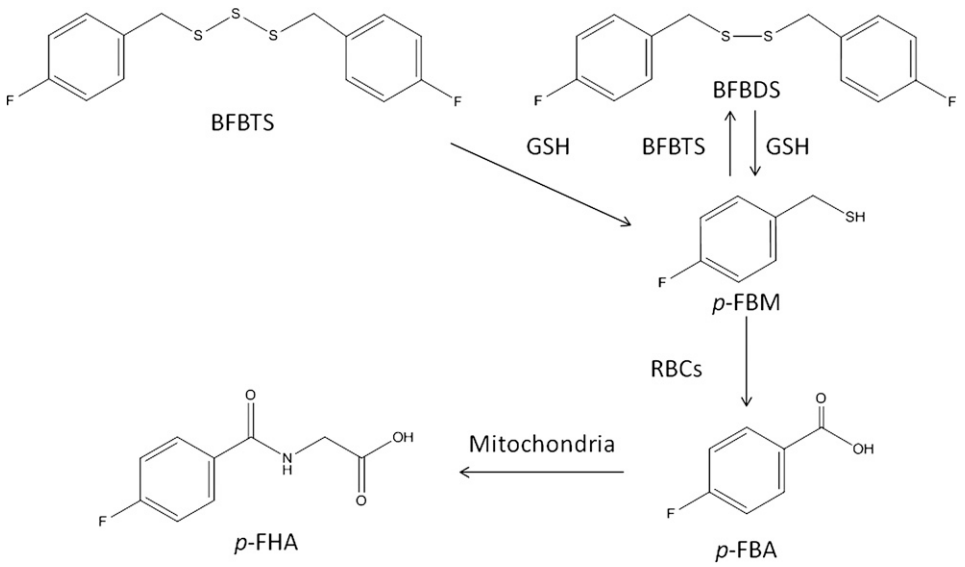

Fig. 10. Pathway of BFBTS metabolism.

to solvent is the highest one among the 5 cysteine residues, thus the steric hindrance for the reaction of BFBTS with Cys125 was negligible. The prevalence of Cys125-modified peptides on β chain revealed that Cys125 was the most reactive site in rat Hb toward BFBTS, which was also consistent with the previous report defining the Cys125 on rat Hb β chain as the fast reacting thiol (Rossi et al., 1998). Cys104/111 on α chain is located internally at the $\alpha 1/\beta 1$ interface(John, 1982); it was suggested that the dissociation of tetramers into dimers will give access to Cys104/111. Cys13 was buried in α chain and Cys93 on β chain was also less exposed to solvent than Cys125, both of which were defined as low-reactive thiol residues. This may be the reason why Cys93-modified peptide was detected only at high concentration (500 μM), while Cys13-modified peptide was not detected.

Apart from the BFBTS-derived adducts, glutathionylation of Hb β chain was observed even more significantly than BFBTS adducts at the same concentration on ESI-TOF. It was well known that the concentration of glutathione-protein mixed disulfide in various rodent tissues increased under oxidative stress(Brigelius et al., 1982, 1983; Keeling et al., 1982; Grimm et al., 1985; Terada et al., 1993; Di Simplicio and Rossi, 1994; Di Simplicio et al., 1996; Giannerini et al., 2001), while the effects of oxidant on blood was found to be more pronounced than other organs in rat(Giannerini et al., 2001).

In our study, glutathionylation of Hb β chain was not found when RBCs was incubated with BFBDS or *p*-FBM but was apparent with BFBTS. Since the extra sulfur atom in the compound will increase its oxidative potential, the obvious glutathionylation of Hb is probably due to the oxidative effect of BFBTS on rat RBCs. Our previous observation of interaction between GSH and BFBTS indicated that the unstable intermediate GSH-*p*-FBM might interact with hemoglobin by the same mechanism. Thus the glutathionylation of Hb β may be ascribed to the oxidative effect of BFBTS or the complicated thiol exchange among GSH, BFBTS, and hemoglobin.

A further investigation of Hb adducts was conducted through in vivo study on rats at a single i.v. dose of 50 mg/kg (Gu et al., 2008). The reason why neither BFBTS-derived adducts nor glutathionylated adducts were detected was probably that the fast elimination induced by GSH resulted in relatively low exposure of BFBTS toward Hb in vivo.

The formation of hemoglobin adducts was also assessed in humans by incubating human RBCs with BFBTS. In this case, hemoglobin adducts were not detected, which indicated a lower risk in forming BFBTS-derived Hb adducts in human.

In summary, we demonstrated the mechanism of BFBTS metabolism in rat RBCs and indicated that rat RBCs were the main site for the metabolism of BFBTS. The main metabolites were identified as BFBDS, *p*-FBM, and *p*-FBA; *p*-FBA was the terminal metabolite, whereas BFBDS and *p*-FBM were the intermediate metabolites. The proposed pathway of BFBTS metabolism is shown in Fig. 10. Thiols were identified as the key factor in the metabolism of BFBTS, whereas the small thiols played a significant role based on the mechanism of thiol exchange reaction. Hemoglobin adducts could be found only in rat RBCs incubated with BFBTS at high concentration on which Cys 125 showed the highest reactivity toward BFBTS. Moreover, no Hb adduct was detected neither in vivo even at a single high i.v. dose of BFBTS in rat nor in human RBCs incubated with BFBTS. Therefore, it can be deduced that the risk of formation of BFBTS adducts is very low at therapeutical exposure of BFBTS.

Acknowledgments

The authors thank Xiaoqiong Ma and Dr. Narenmandura for help with the ESI-TOF MS analysis.

Authorship Contributions

Participated in research design: Pan, Gu, Zeng, Jiang.

Conducted experiments: Pan, Gu.

Contributed new reagents or analytic tools: Pan, Gu, Sun, Chen, Zhou, Zeng, Jiang.

Performed data analysis: Pan, Gu, Sun, Chen, Zhou, Zeng, Jiang.

Wrote or contributed to the writing of the manuscript: Pan, Sun, Jiang.

References

Agarwal KC (1996) Therapeutic actions of garlic constituents. *Med Res Rev* **16**:111–124.

Amagase H (2006) Clarifying the real bioactive constituents of garlic. *J Nutr* **136**(3, Suppl) 716S–725S.

Amagase H, Petesch BL, Matsuura H, Kasuga S, and Itakura Y (2001) Intake of garlic and its bioactive components. *J Nutr* **131** (3s):955S–962S.

An H, Zhu J, Wang X, and Xu X (2006) Synthesis and anti-tumor evaluation of new trisulfide derivatives. *Bioorg Med Chem Lett* **16**:4826–4829.

Bao Y, He Y, Xu X, Mo X, Xu X, Wang X, and An H (2008) Quantitative determination of anti-tumor agent bis(4-fluorobenzyl)trisulfide, fluorapacin and its pharmaceutical preparation by high-performance liquid chromatography. *J Pharm Biomed Anal* **46**:206–210.

Brigelius R, Lenzen R, and Sies H (1982) Increase in hepatic mixed disulphide and glutathione disulphide levels elicited by paraquat. *Biochem Pharmacol* **31**:1637–1641.

Brigelius R, Muckel C, Akerboom TP, and Sies H (1983) Identification and quantitation of glutathione in hepatic protein mixed disulfides and its relationship to glutathione disulfide. *Biochem Pharmacol* **32**:2529–2534.

Di Simplicio P, Cacace MG, Lusini L, Giannerini F, Giustarini D, and Rossi R (1998) Role of protein -SH groups in redox homeostasis—the erythrocyte as a model system. *Arch Biochem Biophys* **355**:145–152.

Di Simplicio P, Lupis E, and Rossi R (1996) Different mechanisms of formation of glutathione-protein mixed disulfides of diamide and tert-butyl hydroperoxide in rat blood. *Biochim Biophys Acta* **1289**:252–260.

Di Simplicio P and Rossi R (1994) The time-course of mixed disulfide formation between GSH and proteins in rat blood after oxidative stress with tert-butyl hydroperoxide. *Biochim Biophys Acta* **1199**:245–252.

Eyer P, Lierheimer E, and Strosar M (1983) Site and mechanism of covalent binding of 4-dimethylaminophenol to human hemoglobin, and its implications to the functional properties. *Mol Pharmacol* **24**:282–290.

Ferranti P, Carbone V, Sannolo N, Fiume I, and Malorni A (1993) Mass spectrometric analysis of rat hemoglobin by FAB-overlapping. Primary structure of the alpha-major and of four beta constitutive chains. *Int J Biochem* **25**:1943–1950.

Fukao T, Hosono T, Misawa S, Seki T, and Ariga T (2004) The effects of allyl sulfides on the induction of phase II detoxification enzymes and liver injury by carbon tetrachloride. *Food Chem Toxicol* **42**:743–749.

Germain E, Chevalier J, Siess MH, and Teyssier C (2003) Hepatic metabolism of diallyl disulphide in rat and man. *Xenobiotica* **33**:1185–1199.

Giannerini F, Giustarini D, Lusini L, Rossi R, and Di Simplicio P (2001) Responses of thiols to an oxidant challenge: differences between blood and tissues in the rat. *Chem Biol Interact* **134**: 73–85.

Giustarini D, Milzani A, Dalle-Donne I, and Rossi R (2008) Red blood cells as a physiological source of glutathione for extracellular fluids. *Blood Cells Mol Dis* **40**:174–179.

Grimm LM, Collison MW, Fisher RA, and Thomas JA (1985) Protein mixed-disulfides in cardiac cells. S-thiolation of soluble proteins in response to diamide. *Biochim Biophys Acta* **844**:50–54.

Gu L, Li L, Chen Z, Pan H, Jiang H, Zeng S, Xu X, and An H (2008) Determination of anti-tumor agent bis(p-fluorobenzyl)trisulfide and its degraded compound in rat blood using reversed phase high-performance liquid chromatography. *J Chromatogr B Analyt Technol Biomed Life Sci* **868**:77–82.

Guan X, Hoffman B, Dwivedi C, and Matthees DP (2003) A simultaneous liquid chromatography/mass spectrometric assay of glutathione, cysteine, homocysteine and their disulfides in biological samples. *J Pharm Biomed Anal* **31**:251–261.

Hosono T, Fukao T, Ogihara J, Ito Y, Shiba H, Seki T, and Ariga T (2005) Diallyl trisulfide suppresses the proliferation and induces apoptosis of human colon cancer cells through oxidative modification of beta-tubulin. *J Biol Chem* **280**:41487–41493.

Iciek M, Marcinek J, Mleczko U, and Włodek L (2007) Selective effects of diallyl disulfide, a sulfane sulfur precursor, in the liver and Ehrlich ascites tumor cells. *Eur J Pharmacol* **569**: 1–7.

Iversen R, Andersen PA, Jensen KS, Winther JR, and Sigurskjold BW (2010) Thiol-disulfide exchange between glutaredoxin and glutathione. *Biochemistry* **49**:810–820.

John ME (1982) Structural, functional and conformational properties of rat hemoglobins. *Eur J Biochem* **124**:305–310.

Keeling PL, Smith LL, and Aldridge WN (1982) The formation of mixed disulphides in rat lung following paraquat administration. Correlation with changes in intermediary metabolism. *Biochim Biophys Acta* **716**:249–257.

Kemp M, Go YM, and Jones DP (2008) Nonequilibrium thermodynamics of thiol/disulfide redox systems: a perspective on redox systems biology. *Free Radic Biol Med* **44**:921–937.

Kim YA, Xiao D, Xiao H, Powolny AA, Lew KL, Reilly ML, Zeng Y, Wang Z, and Singh SV (2007) Mitochondria-mediated apoptosis by diallyl trisulfide in human prostate cancer cells is associated with generation of reactive oxygen species and regulated by Bax/Bak. *Mol Cancer Ther* **6**:1599–1609.

Makheja AN and Bailey JM (1990) Antiplatelet constituents of garlic and onion. *Agents Actions* **29**:360–363.

Moll TS, Harms AC, and Elfarra AA (2000) A comprehensive structural analysis of hemoglobin adducts formed after in vitro exposure of erythrocytes to butadiene monoxide. *Chem Res Toxicol* **13**:1103–1113.

Pan H, Zhou H, Zeng S, Xu X, An H, and Jiang H (2009) Identification and simultaneous determination of p-FHA and p-FBA, two metabolites of anti-tumor agent—Fluorapacin in rat urine. *J Chromatogr B Analyt Technol Biomed Life Sci* **877**:1553–1560.

Rösner H, Williams LA, Jung A, and Kraus W (2001) Disassembly of microtubules and inhibition of neurite outgrowth, neuroblastoma cell proliferation, and MAP kinase tyrosine dephosphorylation by dibenzyl trisulphide. *Biochim Biophys Acta* **1540**:166–177.

Rossi R, Barra D, Bellelli A, Boumis G, Canofeni S, Di Simplicio P, Lusini L, Pascarella S, and Amiconi G (1998) Fast-reacting thiols in rat hemoglobins can intercept damaging species in erythrocytes more efficiently than glutathione. *J Biol Chem* **273**:19198–19206.

Schafer FQ and Buettner GR (2001) Redox environment of the cell as viewed through the redox state of the glutathione disulfide/glutathione couple. *Free Radic Biol Med* **30**:1191–1212.

Seki T, Hosono T, Hosono-Fukao T, Inada K, Tanaka R, Ogihara J, and Ariga T (2008) Anticancer effects of diallyl trisulfide derived from garlic. *Asia Pac J Clin Nutr* **17** (Suppl 1): 249–252.

Simkin JL and White K (1957) The formation of hippuric acid; the influence of benzoate administration on tissue glycine levels. *Biochem J* **65**:574–582.

Sumiyoshi H and Wargovich MJ (1990) Chemoprevention of 1,2-dimethylhydrazine-induced colon cancer in mice by naturally occurring organosulfur compounds. *Cancer Res* **50**: 5084–5087.

Sun X, Guo T, He J, Zhao M, Yan M, Cui F, and Deng Y (2006) Determination of the concentration of diallyl trisulfide in rat whole blood using gas chromatography with electron-capture detection and identification of its major metabolite with gas chromatography mass spectrometry. *Yakugaku Zasshi* **126**:521–527.

Terada T, Nishimura M, Oshida H, Oshida T, and Mizoguchi T (1993) Effect of glucose on thioltransferase activity and protein mixed disulfides concentration in GSH-depleting reagents treated rat erythrocytes. *Biochem Mol Biol Int* **29**:1009–1014.

Teyssier C, Guenot L, Suschetet M, and Siess MH (1999) Metabolism of diallyl disulfide by human liver microsomal cytochromes P-450 and flavin-containing monooxygenases. *Drug Metab Dispos* **27**:835–841.

Teyssier C and Siess MH (2000) Metabolism of dipropyl disulfide by rat liver phase I and phase II enzymes and by isolated perfused rat liver. *Drug Metab Dispos* **28**:648–654.

Wang HC, Hsieh SC, Yang JH, Lin SY, and Sheen LY (2012) Diallyl trisulfide induces apoptosis of human basal cell carcinoma cells via endoplasmic reticulum stress and the mitochondrial pathway. *Nutr Cancer* **64**:770–780.

Wargovich MJ, Woods C, Eng VW, Stephens LC, and Gray K (1988) Chemoprevention of N-nitrosomethylbenzylamine-induced esophageal cancer in rats by the naturally occurring thioether, diallyl sulfide. *Cancer Res* **48**:6872–6875.

Warshafsky S, Kamer RS, and Sivak SL (1993) Effect of garlic on total serum cholesterol. A meta-analysis. *Ann Intern Med* **119**:599–605.

Williams LA, Rösner H, Möller W, Conrad J, Nkurunziza JP, and Kraus W (2004) In vitro anti-proliferation/cytotoxic activity of sixty natural products on the human SH-SY5Y neuroblastoma cells with specific reference to dibenzyl trisulphide. *West Indian Med J* **53**: 208–219.

Xiao D and Singh SV (2006) Diallyl trisulfide, a constituent of processed garlic, inactivates Akt to trigger mitochondrial translocation of BAD and caspase-mediated apoptosis in human prostate cancer cells. *Carcinogenesis* **27**:533–540.

Xu W, Xi B, Wu J, An H, Zhu J, Abassi Y, Feinstein SC, Gaylord M, Geng B, and Yan H, et al. (2009) Natural product derivative Bis(4-fluorobenzyl)trisulfide inhibits tumor growth by modification of beta-tubulin at Cys 12 and suppression of microtubule dynamics. *Mol Cancer Ther* **8**:3318–3330.

Yeh YY and Yeh SM (1994) Garlic reduces plasma lipids by inhibiting hepatic cholesterol and triacylglycerol synthesis. *Lipids* **29**:189–193.

Zeng T, Zhang CL, Zhu ZP, Yu LH, Zhao XL, and Xie KQ (2008) Diallyl trisulfide (DATS) effectively attenuated oxidative stress-mediated liver injury and hepatic mitochondrial dysfunction in acute ethanol-exposed mice. *Toxicology* **252**:86–91.

Zhou Z, Tan HL, Xu BX, Ma ZC, Gao Y, and Wang SQ (2005) Microarray analysis of altered gene expression in diallyl trisulfide-treated HepG2 cells. *Pharmacol Rep* **57**:818–823.

Zimmerman LJ, Valentine HS, Amarnath K, and Valentine WM (2002) Identification of a S-hexahydro-1H-azepine-1-carbonyl adduct produced by molinate on rat hemoglobin beta(2) and beta(3) chains in vivo. *Chem Res Toxicol* **15**:209–217.

Address correspondence to: Dr. Huidi Jiang, Department of Pharmaceutical Analysis and Drug Metabolism, Pharmaceutical Sciences, Zhejiang University, Hangzhou 310058, China. E-mail: hdjiang@zju.edu.cn